Submitted to the Journal of Geophysical Research

LBL-9327 C. 2
Preprint

FAULT ZONE CONTROLLED CHARGING OF A LIQUID DOMINATED GEOTHERMAL RESERVOIR

K. P. Goyal and D. R. Kassoy

RECEIVED
LAWRENCE
BERKELEY LABORATORY

JUL 30 1979

LIBRARY AND
DOCUMENTS SECTION

July 1979

Prepared for the U. S. Department of Energy
under Contract W-7405-ENG-48

TWO-WEEK LOAN COPY

This is a Library Circulating Copy which may be borrowed for two weeks. For a personal retention copy, call Tech. Info. Division, Ext. 6782

LAWRENCE BERKELEY LABORATORY
UNIVERSITY OF CALIFORNIA
BERKELEY

LBL-9327 c. 2

DISCLAIMER

This document was prepared as an account of work sponsored by the United States Government. While this document is believed to contain correct information, neither the United States Government nor any agency thereof, nor the Regents of the University of California, nor any of their employees, makes any warranty, express or implied, or assumes any legal responsibility for the accuracy, completeness, or usefulness of any information, apparatus, product, or process disclosed, or represents that its use would not infringe privately owned rights. Reference herein to any specific commercial product, process, or service by its trade name, trademark, manufacturer, or otherwise, does not necessarily constitute or imply its endorsement, recommendation, or favoring by the United States Government or any agency thereof, or the Regents of the University of California. The views and opinions of authors expressed herein do not necessarily state or reflect those of the United States Government or any agency thereof or the Regents of the University of California.

FAULT ZONE CONTROLLED CHARGING OF A LIQUID DOMINATED GEOTHERMAL RESERVOIR

K.P. Goyal* and D.R. Kassoy
Mechanical Engineering Department

University of Colorado
Boulder, Colorado 80309

A mathematical model is developed for the fault zone controlled charging of a geothermal reservoir. The model is used to describe a reservoir of finite vertical extent with an impermeable upper boundary. A quasianalytic theory is developed for high Rayleigh number convection of liquid in a rigid porous medium. In this approximation, liquid rises up the fault and spreads into the near regions of the reservoir isothermally. The cooling effect of the surface on the fault flow is confined to a thin layer near the surface. This layer grows with distance from the fault. In the far field of the aquifer the full depth of the reservoir is cooled by the surface. A study is made of the effect of various parameters such as mass flow rate, Rayleigh number, and fault width on the pressures, velocities, temperatures and their gradients at different locations in the fault and in the aquifer. This analysis can be applied to geothermal systems where the thickness of the impermeable reservoir cap is quite small compared to the reservoir depth.

1. Introduction

In recent years mathematical models of heat and mass transfer in unexploited liquid-dominated geothermal systems have evolved from the extremely idealized variety into a form which is at least physically viable. As geophysical field data from a multitude of systems was collected and analysed it has become possible to develop conceptual reservoir models which contain elements of physical plausibility. The latter property has not always been present in modeling efforts. For instance the category of hypothetical idealized models, represented by extensions of classical hydrodynamic stability theory in porous

*Present address: Earth Sciences Division, Lawrence Berkeley Laboratory, UC Berkeley, California 94720

media (see review articles by Combarnous and Bories [1975], Cheng [1978], Garg and Kassoy [1979]) lacks both the significant internal structure and the boundary conditions relevant to real geothermal systems. These models can be used to develop the fundamental principles of convection processes and even to find semi-quantitative estimates of the magnitudes of heat and mass transfer in field situations. Yet their configuration and properties preclude the comparison of theoretical prediction with field measurements. In addition elements of hydrodynamical stability, which appear as a result of an incompletely defined system (infinite slab configuration) or simplified thermal boundary condition (uniform temperature on a horizontal boundary), tend to introduce specicous physical effects which probably do not arise in real systems. As an example the convection mode observed in the field is almost surely the result of geological structure (the combination of fracture zones, faults, aquifers) rather than hydrodynamic stability properties.

Hypothetical but more plausible models which contain elements of configurational, structural and thermal reality, were introduced by Einarsson [1942], Wooding [1957] and Elder [1966]. The first author's pipe model concept arises from on the hydrostatic imbalance that exists between the heated, low density water in the active part of a geothermal reservoir and the colder, denser water in the peripheral region. Qualitative properties of these global geothermal systems were discussed by Elder [1966], Bodvarsson [1961] and White [1961]. A quantitative study is given by Donaldson [1968, 1970].

The large scale convection cell models of Cheng and co-workers, summarized in Cheng [1978] represent a second type of plausible model. In a typical example Cheng and Teckchandani [1977] investigate the time-history of a convection pattern initiated by a distributed hot spot on the lower boundary of a completely defined reservoir region. In a related fashion Norton [1977], Norton and Knight [1977], Cathles [1977] and Torrence and Sheu [1978] have examined the evolution of a convection system caused by the emplacement of an intrusive or pluton in a water-saturated fractured rock system.

Other plausible models concentrate on smaller-scale geological configurations. Sorey [1975] and Turcotte, Ribando and Torrence [1977], and Kassoy and Zebib [1978], have generated distinctly different models for hot springs systems based on convection in high permeabilty fracture zones associated with faulting. Heat transfer from a simple model of a dike has been described by Cheng and Minkowicz [1977].

Preproduction models of unexploited systems are based on interpretation and analysis of field data sets. An effort is made to represent the essential physical features of the observed systems in both the conceptual and mathematical sense. Typical examples include Wooding's [1957] cross-sectional model of upflow in the Wairakei system, the two-dimensional areal reservoir model for Wairakei by Mercer, et al. [1975] and Mercer and Faust [1979], Sory's [1976] large-scale vertical model of the Long Valley Caldera, the Salton Sea reservoir areal model developed by Riney et al. [1977] and a vertical analysis of East Mesa System by Goyal [1978].

The present study involves a plausible, hypothetical model for a geothermal reservoir charged by heated water from a vertical fault zone. It is motivated by observations of the East Mesa field in the Imperial Valley, California. A two-dimensional mathematical model of a liquid dominated geothermal system with impermeable upper boundary has been developed. The saturated porous media equations are used to describe this model. The solution techniques involve the combination of perturbation methods, boundary layer theory and numerical methods. Results are presented for the pressures, velocities, temperatures and temperature gradients in the system. The application of this theory to a typical geothermal system is discussed in the last section of this paper.

2. Conceptual Model Development

Recent studies of liquid-dominated geothermal systems like Wairakei [Grindley, 1965], Broadlands [Grindley, 1970], Long Valley [Rinehart and Ross, 1964], Ahuachapan [Ward and Jacobs, 1971], and Imperial Valley [Elders et al, 1972] suggest that geothermal anomalies are intimately associated with specific patterns of faulting. Combs and Hadley [1977] have suggested that the Mesa fault at the East Mesa geothermal anomaly in the Imperial Valley acts as a conduit for hot waters rising from depth. It has been hypothesized [Bailey, 1977] that the geothermal reservoir is generated by charging of hot water from the fault at an intersection with a aquifer of appropriate horizontal permeability. A conceptual model of such a system is shown in Figure 1. The fault is hypothesized to be a vertically oriented region of heavily fractured material of finite width ($2\ y_e'$). The vertical extent and the second horizontal dimension of the fault are large compared to the width. The fault extends

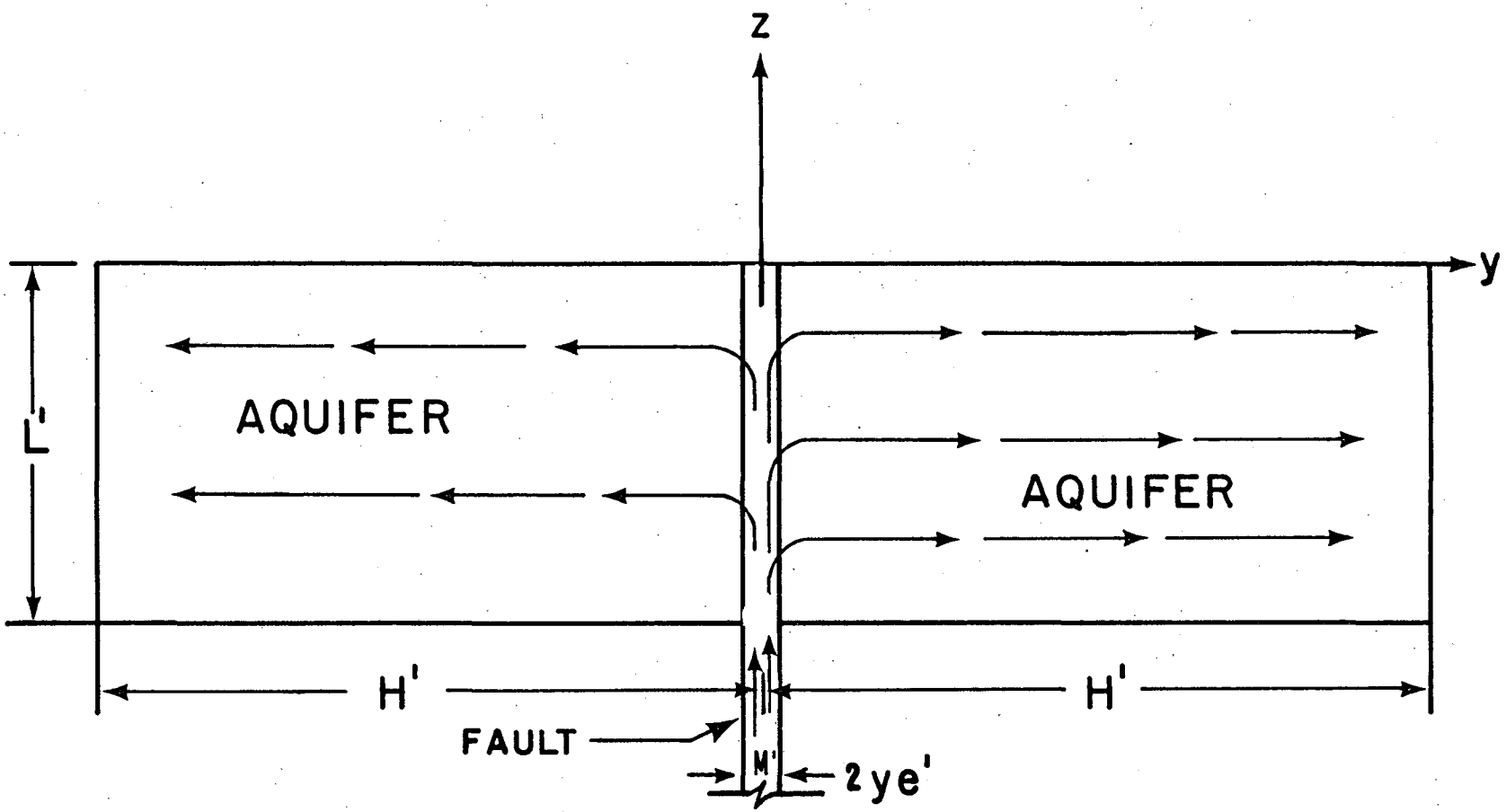

Figure 1. Conceptual Model of a Liquid Dominated Geothermal System.

XBL 7812-2200

downward through the interbedded sediments of the reservoir for a distance L′ and then into the basement rock. It is postulated that the fault is charged at depth by the liquid which has been heated in an extensive basement fractured system. The rate of charge cannot be specified a priori without a global analysis of the convection process. The liquid rises up in the reservoir section of the fault and is pushed into the aquifer by the overpressure associated with the convection process. The liquid is assumed to flow horizontally in the aquifer since general vertical permeability is minimized by the presence of shaley layers associated with interbedding in geothermal systems like those at East Mesa [Bailey, 1977] and at Wairakei [Donaldson, 1978].

For mathematical purposes, the fracture zone is idealized as a vertical slab of porous media. The adjacent aquifer is represented as a porous medium of lateral half width H′ with horizontal permeability only. Spatially uniform temperature boundary conditions are imposed on the cold top surface and at the hot bottom boundary of the reservoir. As a result, far from the fault the horizontal temperature gradient becomes vanishingly small even though the horizontal motion of the liquid persists. The temperature distribution at a vertical boundary in this region will be controlled essentially by the vertical conduction. The horizontal location of this boundary ($y' = H'$) is specified during the calcuations by locating a position where the horizontal heat flux is small compared to that in the vertical direction. The associated hydrostatic pressure distribution at the far field boundary can be calculated once the density distribution is known.

It is to be emphasized that this model is only a part of a "global circulation pattern." It does not define the downflow and heat-up zones, and thus input mass cannot be specified. The driving mechanism for the convection, the result of a hydrostatic pressure imbalance between the hot upflow region and the cold downflow zone, is identical to that envisioned by Donaldson [1968].

3. Mathematical Model

A detailed derivation of the describing equations for a thermally active saturated, deformable porous material is given by Goyal [1978]. The equations used in the present study are obtained from that set by assuming that the flow is steady, the solid matrix is rigid, the fault medium is homogeneous and isotropic, liquid properties are constant, the thermal conductivities of the

fault and aquifer media are constant and equal, and that the vertical permeability in the aquifer is much smaller than the horizontal value, which is equal to that of the fault. In addition the Boussinesq approximation is invoked.

The describing dimensional equations are:

Fault zone:

$$V'_{y'} + W'_{z'} = 0 \tag{1}$$

$$V' = -\frac{K'}{\nu'} P'_{y'} \tag{2}$$

$$W' = \frac{K'}{\nu'} \{-(P' - p'_H)_{z'} + g'(\rho' - \rho'_o)\} \tag{3}$$

$$C'_p \{V' T'_{y'} + W' T'_{z'}\} = \lambda'_m \{T'_{y'y'} + T'_{z'z'}\} \tag{4}$$

$$\rho' = \rho'_o [1 - \alpha'_e (T' - T'_o)] \tag{5}$$

Aquifer:

$$v'(z') = -\frac{K'}{\nu'} p'_{y'} \tag{6}$$

$$C'_p v' \theta'_{y'} = \lambda'_m (\theta'_{y'y'} + \theta'_{z'z'}) \tag{7}$$

where the variables are defined below eqation (18). The solution of the above system is subjected to the following boundary and continuity conditions.

Boundary conditions:

Fault zone:

$$W'(y',0) = 0, \quad \text{impermeable upper boundary} \tag{8}$$

$$\int_{-y_e'}^{+y_e'} W'(y', -L')\, dy' = M', \quad \text{input mass flow rate} \tag{9}$$

$$T'(y', 0) = T'_o, \quad \text{cold upper boundary} \tag{10}$$

$$T'(y', -L') = T'_{max}, \quad \text{hot lower boundary} \tag{11}$$

$$T'_{y'}(0, z') = 0, \quad \text{symmetry} \tag{12}$$

Aquifer:

$$\theta'(y', 0) = T'_o, \qquad \text{cold upper boundary} \qquad (13)$$

$$\theta'(y', -L') = T'_{max}, \qquad \text{hot lower boundary} \qquad (14)$$

$$\theta'(H', z') = T'_o - (T'_{max} - T'_o)\frac{z'}{L'}, \qquad \text{aquifer edge} \qquad (15)$$

Equation (15) is a formal statement of the required conduction - controlled heat transfer at the far-field boundary. The value of H' is found in the course of analysis.

Continuity conditions at the fault-aquifer boundary:

$$T'(y_e', z') = \theta'(y_e', z') \qquad (16)$$

$$V'(\pm y_e', z') = \pm v'(z') \qquad (17)$$

$$P'(y_e', z') = p'(y_e', z') \qquad (18)$$

The dimensional variables are defined by

V' = horizontal Darcy mass flux in the fault per unit area, gm/cm^2 - sec

W' = vertical Darcy mass flux in the fault per unit area, gm/cm^2 - sec

K' = fault permeability and horizontal permeability in the aquifer, cm^2

ν' = kinematic viscosity, cm^2/sec

P' = fault pressure, $dynes/cm^2$

p'_H = cold hydrostatic pressure with respect to density ρ'_o, $dynes/cm^2$

ρ'_o = density of the liquid at the ambient temperature T'_o, gm/cm^3

ρ' = density of the liquid at the temperature T', gm/cm^3

g' = acceleration due to gravity, cm/sec^2

C_p' = specific heat of the liquid at constant pressure, cm^2/sec^2-^oK

T' = fault temperature, ^oK

λ_m' = medium thermal conductivity, gm - cm/sec^3 - ^oK

α_e' = coefficient of thermal expansion of the liquid, /^oK

T_o' = ambient temperature, ^oK

v' = horizontal mass flux in the aquifer per unit area, gm/cm^2-sec

p' = aquifer pressure, dynes /cm^2

θ' = aquifer temperature, ^oK

y_e' = semifault width, cm

L' = depth of the reservoir, cm

M' = mass flow rate per unit length in the direction perpendicular to the plane of paper, gm/cm-sec

T_{max}' = maximum temperature at the hot bottom boundary of the reservoir, ^oK

In the fault, where the characteristic horizontal dimension and velocity component are much smaller than their vertical counterparts, the appropriate nondimensional variables can be defined as:

$$\bar{y} = y'/y_e', \quad y_e = y_e'/L', \quad z = z'/L'$$

$$\bar{V} = V'/y_e q_o' \rho_o', \quad W = W'/q_o'\rho_o', \quad T = T'/T_o', \tag{19}$$

$$\tau = (T_{max}' - T_o')/T_o', \quad P = (P' - p_H')/p_o',$$

Substitution of (19) into (1)-(7) leads to an inherent balance between the buoyancy, Darcy, and pressure terms in the vertical momentum equation, if

$$q_o' = \frac{\alpha_e' \quad \Delta T' g' K'}{\nu'} = \text{reference convection velocity}$$

$$p_o' = \rho_o' g' \alpha_e' L' \Delta T' = \text{reference convection pressure} \tag{20}$$

$$R = \frac{\rho'_o q'_o C'_p \Delta T'}{\lambda'_m (\Delta T'/L')} = \text{Rayleigh number}$$

where $\Delta T' = T'_{Max} - T'_o$

The nondimensional equations, transformed boundary and continuity conditions relevant in the fault zone can be written as

Fault zone:

$$\overline{V}_{\bar{y}} + W_z = 0 \tag{21}$$

$$y_e^2 \, \overline{V} = - P_{\bar{y}} \tag{22}$$

$$W = - P_z + (T-1)/\tau \tag{23}$$

$$\gamma^2 \, (\overline{V} T_{\bar{y}} + W T_z) = T_{\bar{y}\bar{y}} + y_e^2 \, T_{zz} \tag{24}$$

$$\gamma = R^{1/2} \, y_e \tag{25}$$

$$W(\bar{y}, 0) = 0 \tag{26}$$

$$W(\bar{y}, -1) = M \tag{27}$$

$$M = M'/M'_o, \quad M'_o = 2 \, y_e' \, \rho'_o \, q'_o \tag{28a,b}$$

$$T(\bar{y}, 0) = 1 \tag{29}$$

$$T(\bar{y}, -1) = 1 + \tau \tag{30}$$

$$T_{\bar{y}} \, (0,z) = 0 \tag{31}$$

$$V(\pm 1, z) = \pm \, v(z) \tag{32}$$

In the aquifer where the horizontal scale is measured by $\hat{y} = y'/H'$, the pressure $p = P_{,}$, the temperature $\theta = T$, and the velocity $v = V$, the appropriate system of equations is given by:

Aquifer:

$$v(z) = -p_{\hat{y}}/d \tag{33}$$

$$d\gamma^2 \; v(z)\theta_{\hat{y}} = y_e^2 \; \theta_{\hat{y}\hat{y}} + d^2\theta_{zz} \tag{34}$$

where

$$H'/L' = d/y_e, \; d = O(1) \text{ number} \tag{35a,b}$$

$$\theta(\hat{y}, 0) = 1 \tag{36}$$

$$\theta(\hat{y}, -1) = 1 + \tau \tag{37}$$

$$\theta(\hat{y} = y_e^2/d, z) = T(\bar{y} = 1, z) \tag{38}$$

$$\theta(\hat{y} = 1, z) = 1 - \tau z \tag{39}$$

The magnitude of H' with respect to the fault depth, L', given in (35) is chosen to ensure a balance between the nondimensional aquifer velocity v and the horizontal pressure gradient as shown in (33). The specific value of d is found in the course of analysis.

In order to proceed further we must consider the magnitude of the Rayleigh number and the parameter γ. If parameter values typical of geothermal systems ($K' = 10^{-13}$ m^2 and thermodynamic variables evaluated at $T_o' = 298$ ^oK) are used in (19) and (20) we find that

$$3\text{x}10^5 \text{ Pa} \lesssim p_o' \lesssim 15 \text{ x } 10^5 \text{ Pa}$$

$$10^{-2} \text{ m/day} \lesssim q_o' \lesssim 10^{-1} \text{ m/day}$$

$$0.2 \lesssim \tau \lesssim 1$$

$$2\text{x}10^2 \lesssim R \lesssim 10^4$$

Large values of R suggest that energy transfier associated with liquid convection is far greater than that due to conduction. In this regard one may expect that fluid particles moving through the system will tend to behave isothermally unless affected by cooling associated with a relatively cold boundary.

The parameter γ is assumed to be an 0(1) number because y_e is considered small. If for instance we consider $R = 10^3$ and $L' = 2$km then $y_e' = 63.2\gamma$ meters, indicating that reasonable fault zone thicknesses can be incorporated in the theory. In the mathematical analysis solutions are sought in the limit of large R with $\gamma = 0(1)$ implying, of course that y_e is small.

The cooling effect of the surface is confined to a thin thermal boundary layer near the top of the fault for a high Rayleigh number flow. The boundary layer grows as the fluid moves away from the fault and virtually occupies the whole depth of the aquifer in the far field. Thus, the flow outside the boundary layer is an isothermal flow.

It can be noted from (22) that the horizontal pressure gradient in the fault is very small, $0(ye^2)$. Thus, the basic fault pressure is only a function of depth and can be calculated in terms of W and v. The horizontal aquifer velocity v(z) can then be calculated explicitly from (33) because the far field pressure is known once (39) is specified. Upon decoupling the fluid mechanics from the thermal problem, the energy equation (34) can then be solved for the temperatures in the aquifer.

4. Fault Zone Solution

The water in the fault zone rises adiabatically because the convection Rayleigh number is considered to be large. Even the liquid in the aquifer just adjacent to the fault remains at the supply temperature. Cooling in the fault itself can take place only in a thin boundary layer just below the cold upper surface. The uppermost portion of the neighboring aquifer is similarly effected.

The basic solutions in the isothermal portions of the fault and aquifer system are:

$$T = 1 + \tau \tag{40}$$

$$V = \bar{y} \quad \{a_1 \cosh z/\sqrt{d} + b_1 \sinh z/\sqrt{d} - 1\} + 0(y_e{}^2) \tag{41}$$

$$W = - a_1\sqrt{d} \sinh z/\sqrt{d} - \cosh z/\sqrt{d} + z+1 + 0(y_e{}^2) \tag{42}$$

$$P = d\{a_1 \cosh z/\sqrt{d} + b_1 \sinh z/\sqrt{d} -1\} - z^2/2 + 0(y_e{}^2) \tag{43}$$

$$v(z) = a_1 \cosh z/\sqrt{d} + b_1 \sinh z/\sqrt{d} - 1 + 0(y_e{}^2) \tag{44}$$

$$p = v(z)d\ (1-\hat{y}) - z^2/2 + 0(y_e 2) \tag{45}$$

where

$$a_1 = \frac{M + \cosh 1/\sqrt{d}}{\sqrt{d} \sinh 1/\sqrt{d}}\ ,\ b_1 = 1/\sqrt{d} \tag{46a,b}$$

It can be noted that $(-z^2/2)$ is the pressure at the far field boundary of the aquifer and is consistent with the specified temperature field(39).

According to (29), the nondimensional temperature at the top of the fault is 1. There should be a boundary layer to accomodate the temperature drop from $1 + \tau$ to 1. If the appropriately scaled variables

$$\bar{z} = z/y_e \quad \text{and } \bar{W} = W/y_e \tag{47a,b}$$

are used in the basic fault-zone equations then the lowest order boundary layer system has the form:

$$V_{o\bar{y}} + W_{o\bar{z}} = 0 \tag{48}$$

$$P_{1\bar{y}} = 0 \tag{49}$$

$$\frac{T_o - 1}{\tau} - P_{1\bar{z}} = 0 \tag{50}$$

$$\gamma^2(V_o T_{o\bar{y}} + W_o T_{o\bar{z}}) = T_{o\bar{y}\bar{y}} + T_{o\bar{z}\bar{z}} \tag{51}$$

However, it can easily be seen that the lowest order fault pressure p_o is a constant and when matched with the outer solution (43) one finds that

$$P_o = d(a_1 - 1) \tag{52}$$

The solution to the system of equations (48) to (51) is subjected to the following boundary, matching and continuity conditions.

$$T_o(\bar{y}, 0) = 1 \tag{53}$$

$$T_o(\bar{y}, \bar{z} \to -\infty) = 1 + \tau \tag{54}$$

$$W_o(\bar{y}, \bar{z} \to 0) = 0 \tag{55}$$

$$W_o(\bar{y}, \bar{z} \to -\infty) = -\bar{z}(a_1 - 1) \tag{56}$$

$$P_1(\bar{y}, \bar{z} \to -\infty) = \bar{z} \tag{57}$$

It can be noted that the matching conditions ($\bar{z} \to -\infty$) are obtained from the outer solutions (40) - (43). The boundary layer solutions can be written as:

$$\bar{V} = (a_1 - 1)\bar{y} + 0(y_e) \tag{58}$$

$$\bar{W} = -(a_1 - 1)\bar{z} + 0(y_e) \tag{59}$$

$$T = 1 - \tau \operatorname{erf}(A\bar{z}) + 0(y_e) \tag{60}$$

$$P = d(a_1 - 1) - y_e\{\bar{z} \operatorname{erf}(A\bar{z}) + \frac{1}{A\sqrt{\pi}} e^{-A^2\bar{z}^2}\} + 0(y_e^2) \tag{61}$$

where

$$A = \sqrt{\gamma^2 (a_1 - 1)/2} \tag{62}$$

The thermal boundary layer initiated at the top of the fault continues into the adjacent aquifer over a horizontal distance of scale y_e'. In this initial aquifer zone of water cooling, the relevant equations for the velocity and pressure field are

$$v_o(\bar{z}) = - p_{o\hat{y}}/d \tag{63}$$

The appropriate matching and continuity conditions are expressed as:

$$V_o(\pm 1, \bar{z}) = \pm v_o(\bar{z}) \tag{64}$$

$$v_o(\bar{z} \to -\infty) = a_1 - 1 \tag{65}$$

$$p_o(\hat{y}, z \to -\infty) = d(1 - \hat{y})(a_1 - 1) \tag{66}$$

The solution forms are given by

$$v(\bar{z}) = (a_1 - 1) + 0(y_e) \tag{67}$$

$$p(\hat{y}, \bar{z}) = d(a_1 - 1)(1 - \hat{y}) + 0(y_e) \tag{68}$$

4. Temperature Distributions in the Aquifer

Once the velocity field in the aquifer is known the temperature can be calculated from the energy equation. This must be done for five different regions shown in Figure 2. In the near field, the aquifer energy equation (region 1) can be written as follows:

$$\gamma^2 v(\bar{z})\, \theta_{\bar{y}} = \theta_{\bar{y}\bar{y}} + \theta_{\bar{z}\bar{z}} \tag{69}$$

The equation, describing the thermal boundary layer in the region 3 is:

$$\gamma^2 v(z^*)\, \theta_y = y_e\, \theta_{yy} + \theta_{z^*z^*} \tag{70}$$

where

$$y = y'/L' \text{ and } z^* = z/y_e^{1/2} \tag{71a,b}$$

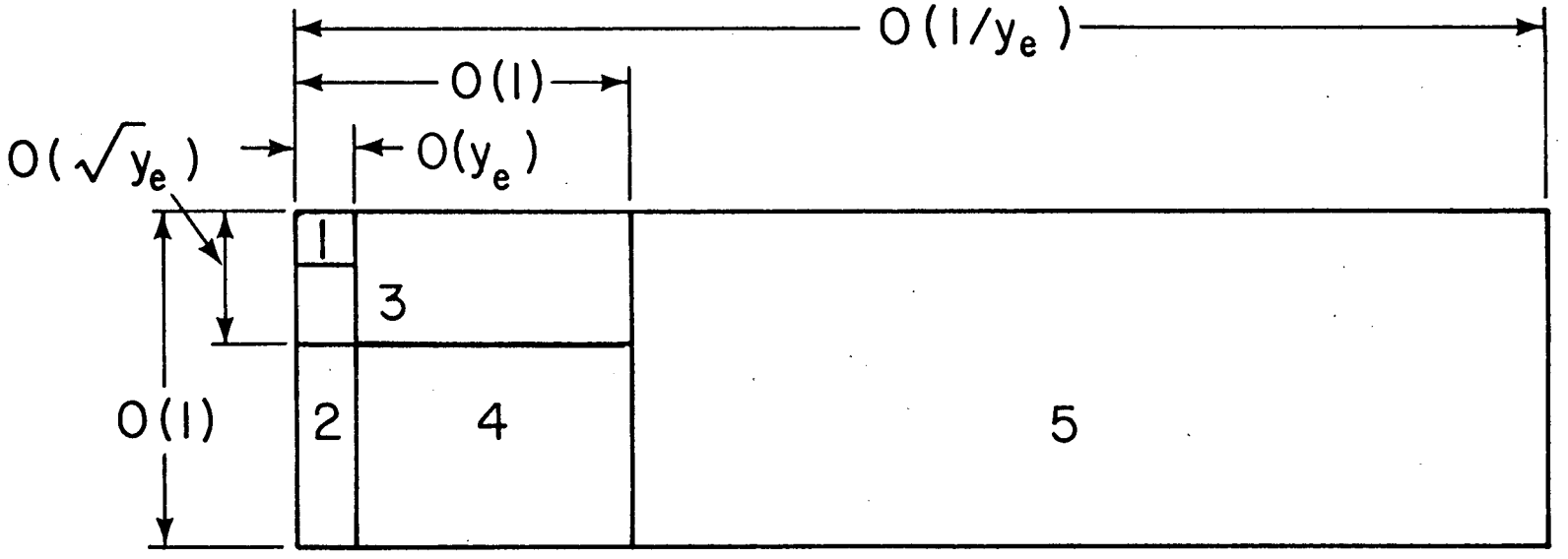

Figure 2. Five Different Regions in the Aquifer.

XBL 796-1978

Since the effect of the surface cooling is limited to the boundary layer regions 1 and 3, the flow in regions 2 and 4 is isothermal. The energy equation in the far field where the full depth of the aquifer is affected by the surface cooling is expressed in terms of $\hat{y}$ and z and is given by (34).

Equation (69) is subjected to the following boundary conditions.

$$\theta(1, \bar{z}) = T(1, \bar{z}) = 1 - \tau \operatorname{erf}(A\bar{z}) \tag{72a}$$

$$\theta(\bar{y} \to \infty, \bar{z}) \quad \text{bounded} \tag{72b}$$

$$\theta(\bar{y}, 0) = 1 \tag{72c}$$

$$\theta(\bar{y}, \bar{z} \to -\infty) = 1 + \tau \tag{72d}$$

Equation (72a) represents the continuity of the temperature at the interface between the fault and the aquifer. The solution in region 1 can be written as

$$\theta(\bar{y}, \bar{z}) = 1 - \frac{2\tau}{\pi} \int_{-\infty}^{0} e^{\left\{ -\frac{\omega^2}{4A^2} - A^2 + \sqrt{A^4 + \omega^2} + (A^2 - \sqrt{A^4 + \omega^2})\,\bar{y} \right\}} \frac{\sin \omega\bar{z}}{\omega}\, d\omega \tag{73}$$

by using the Fourier sine integral transform of θ with respect to $\bar{z}$. When $\bar{y} \to \infty$, the asymptotic form of (73) is

$$\theta(\bar{y}, \bar{z}) = 1 - \sqrt{2/\pi}\ \tau A\, \bar{z}/\bar{y}^{1/2} \tag{74}$$

which indicates that a similarity variable $\bar{z}/\bar{y}^{1/2}$ will be significant in region 3. The thermal boundary layer in the latter region is born in the preceding elliptic region as described formally by Eckhaus [1973].

A similarity solution, compatible with the solution in region 1 can be obtained in the region 3. Elementary methods yield

$$\theta(y,z^*) = 1 - \tau \operatorname{erf}\left(\frac{A}{\sqrt{2}}\eta\right), \quad \eta = z^*/y^{1/2} \tag{75a,b}$$

It is possible to obtain an analytical solution of (34) in region 5, when $\hat{y} << 1$ and $z << 1$, such that $z/\hat{y}^{1/2} = O(1)$, which can be matched with (75a) We find the form

$$\theta(\hat{y},z) = 1 - \tau \operatorname{erf}\left[\frac{A}{\sqrt{2d}}\frac{z}{\hat{y}^{1/2}}\right] + \frac{\hat{y}^{1/2}\ \tau\gamma^2}{4\sqrt{2d}\ A^2}\left[\frac{z}{\sqrt{2d\hat{y}}}\left\{1 + \operatorname{erf}\left(\frac{Az}{\sqrt{2d\hat{y}}}\right)\right\}\right. \tag{76}$$

$$\left. - \frac{Az^2}{d\hat{y}\sqrt{\pi}}\, e^{-\frac{A^2z^2}{2d\hat{y}}}\right] + O(\hat{y})$$

by using coordinate expansion methods. This solution provides the transition between the incompatable conditions $\theta(\hat{y},o) = 1$, $\theta(\hat{y}\to 0,z) = 1 + \tau$ for $|z| > 0$ in the vicinity of the singular corner $\hat{y} = z = 0$.

The energy equation in (34), parabolic to the lowest order, must be solved subject to the boundary conditions in (36) and (37) and the initial condition $\theta(\hat{y}\to 0,z) = 1 + \tau$ for $|z| > 0$ obtained from matching with region 4. The last formal condition at the far end of the aquifer, (39), is used to determine a value for d. Numerical integration by standard finite difference methods is carried out for assumed values of d until the solution at the far edge is within 1% of the real condition. This approximation provides an engineering-type estimate of the boundary location. At that point convection of energy associated with the $\theta_{\hat{y}}$ - term in (34) is very small compared to the conduction term. Of course in the formal mathematical sense, the purely conductive profile can be found only for $\hat{y}\to\infty$.

It is found that d is different for different sets of parameters as listed in Table 1. It can be observed from this table that an increase in M, R, τ, or y_e increases d; which means that a larger aquifer is needed for the transition to the conduction temperature profile when the parameter is increased. In physical terms this result implies that the hot isothermal portions of the aquifer, maintained by horizontal convection effects will be more extensive in

Table 1

d	M	R	τ	ye
<.12	<1	500	1	.025
.12	1	500	1	.025
.3	2	500	1	.025
.47	3	500	1	.025
.64	4	500	1	.025
.47	2	750	1	.025
.64	2	1000	1	.025
.35	2	500	2	.025
1.34	2	500	1	.05

systems of relatively larger mass flow, permeability, temperature difference and fault size. It can also be seen that $M < 1$ gives rise to $H'/L' = 0(1)$ for which this analysis is not valid (35). The solutions for cases $M < 1$ and $d < .12$ were such that at a given location y' the liquid moved away from the fault at some levels and towards it at others.

5. Results

Based on seismic refraction and temperature studies, Combs [1977] predicted the depth of the basement in the East Mesa area to be about 4.15 km and basement-sediment interface temperature of 325°C to 365°C. The thickness of the shaley sediments capping the reservoir is about .8 km [Bailey 1977]. According to this information, the thickness of the reservoir (L') is about 3.35 km. For a temperature difference ($\Delta T'$) of about 300°C across the system and an assumed permeability (K') of 10^{-9} cm^2, we find that

$$R \simeq 580$$

$$\tau \simeq 1$$

Thus the values of R and τ used in the following figures are representative of a typical geothermal system. The value of y_e is a guess but for reasonable fault depth it implies a reasonably thin shear zones. The actual mass flow rate for $M = 1$, is estimated to 12.35×10^5 kg per day per km length of the fault for this set of data. The dimensional mass flow rate for $M = 2$ is equal to 24.7×10^5 kg/day - km.

The dependence of various parameters on the velocity, pressure, temperature, and surface heat flux in the fault and the aquifer is given in figures (3-6). The value of d used in these figures is for the parameters shown.

Figure 3 shows the plots of the vertical velocity and the over-pressure in the fault at various depths for different mass flow rates. Vertical velocity (W) increases with the increase of M, as should be expected. It vanishes at the top of the fault because of the impermeable boundary assumption. All the water is pushed into the aquifer by the time it reaches the top surface of the fault. Overall magnitudes of the overpressure increase with increasing mass flow rate. For high mass flow rates ($M > 2$) over-pressures are highest at the inlet of the fault, decreasing upwards and then again increasing towards the top of the fault. The pressure increase towards the top of the fault is caused

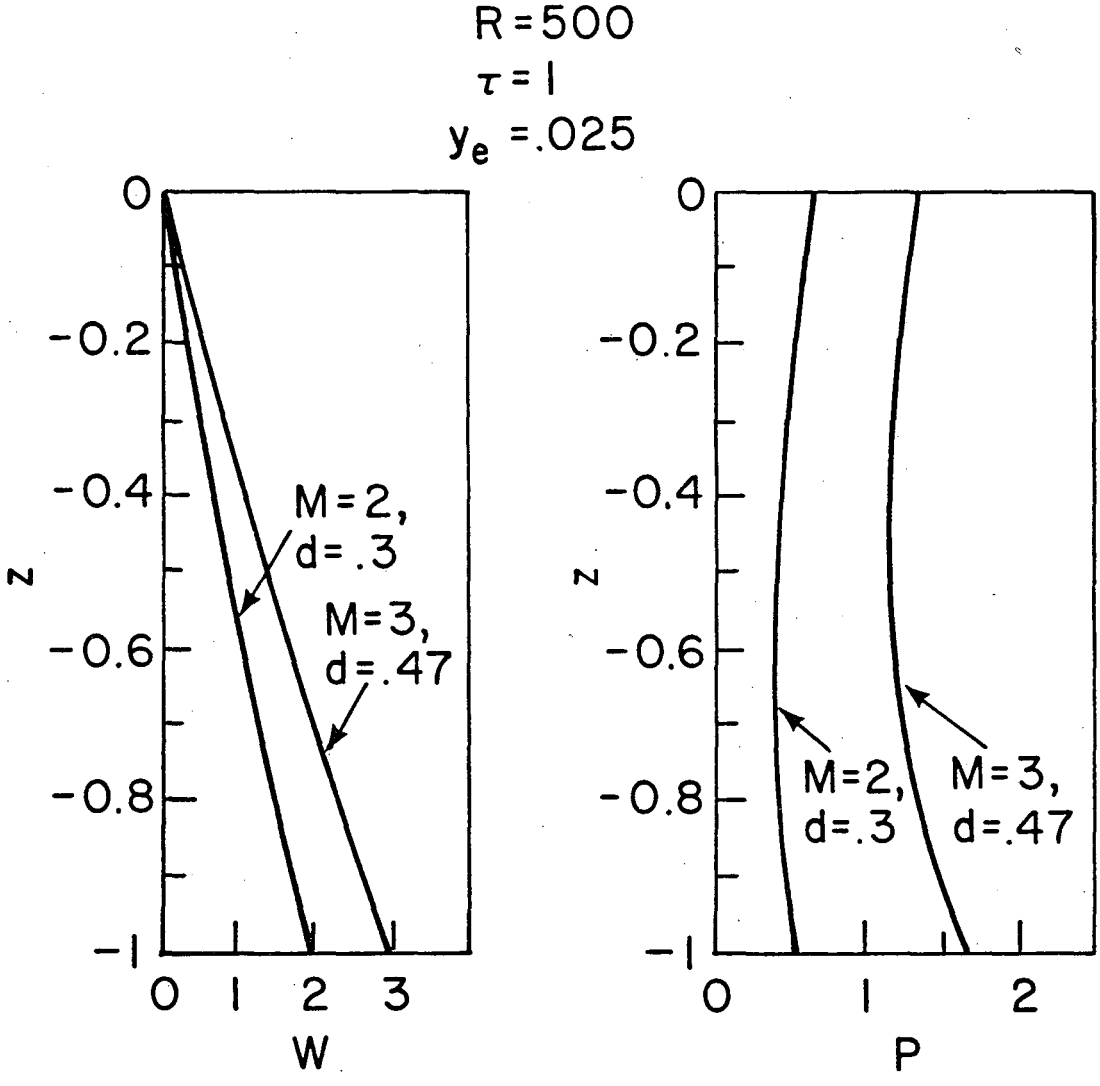

Figure 3. Vertical Velocity Distribution and Over Pressure Along the Depth of the Fault for Different Mass Flow Rates.

XBL 796-1979

by the stagnation point at $z = 0$. The magnitude of the pressures associated with the flow field can be obtained by multiplying the nondimensional pressures of Figure 3 by 25×10^5 Pascals.

Figure 4 shows the fault boundary-layer temperatures for several Rayleigh numbers. It can be noted that the boundary layer thickness decreases with increasing R. This is caused by the increasing effectiveness of convection as R increases. Similar effects are also seen with the increasing mass flow rate.

The horizontal velocity (v) in the aquifer at different depths for several mass flow rates is shown in Figure 5. The trend of curves is similar to the overpressure curves in the Figure 3. The larger velocities at the top of the aquifer are associated with the relatively horizontal higher pressure gradients there.

Figure 6 shows the variation of the aquifer temperature with depth at several horizontal locations. The value $\hat{y} = 1$ represents the far end of the aquifer, which is located at d/ye times its dpeth. The temperature decrease with the increasing distance from the fault can be seen in the aquifer which is affected by the heat loss to the cold upper boundary. It can be noted that at $\hat{y} = 0.1$ half the aquifer is at least within 80% of the high temperature value. The corresponding isotherm map is shown in Figure 7. It is apparent that the horizontal temperature gradient decreases as the liquid moves away from the fault and becomes negligibly small near the far end. Near fault isotherms, also shown in this figure, are calculated from the boundary layer solutions of region 1 and 3.

Figure 8 shows the effect of mass flow rate on the surface temperature gradients both for the fault and the aquifer. Heat transfer at the surface increases with increasing mass flow rate, as expected. Matching of the three regions is shown for $M = 2$. It can be noted that the length of the aquifer is different for each M. This is because of the different value of d associated with a different mass flow rate. It is found that an increase in R, τ, and y_e enhances the temperature grandients at the surface, as expected. The results imply that the fault zone convection process enhances the surface heat flux by a factor of about 30 above the background conductive value.

This value is the right order of magnitude for geothermal systems with vigorous surface manifestations where heated water is present in an extensive region just below the surface. It is rather large for systems exemplified by East Mesa, Imperial Valley, California where the reservoir is separated from

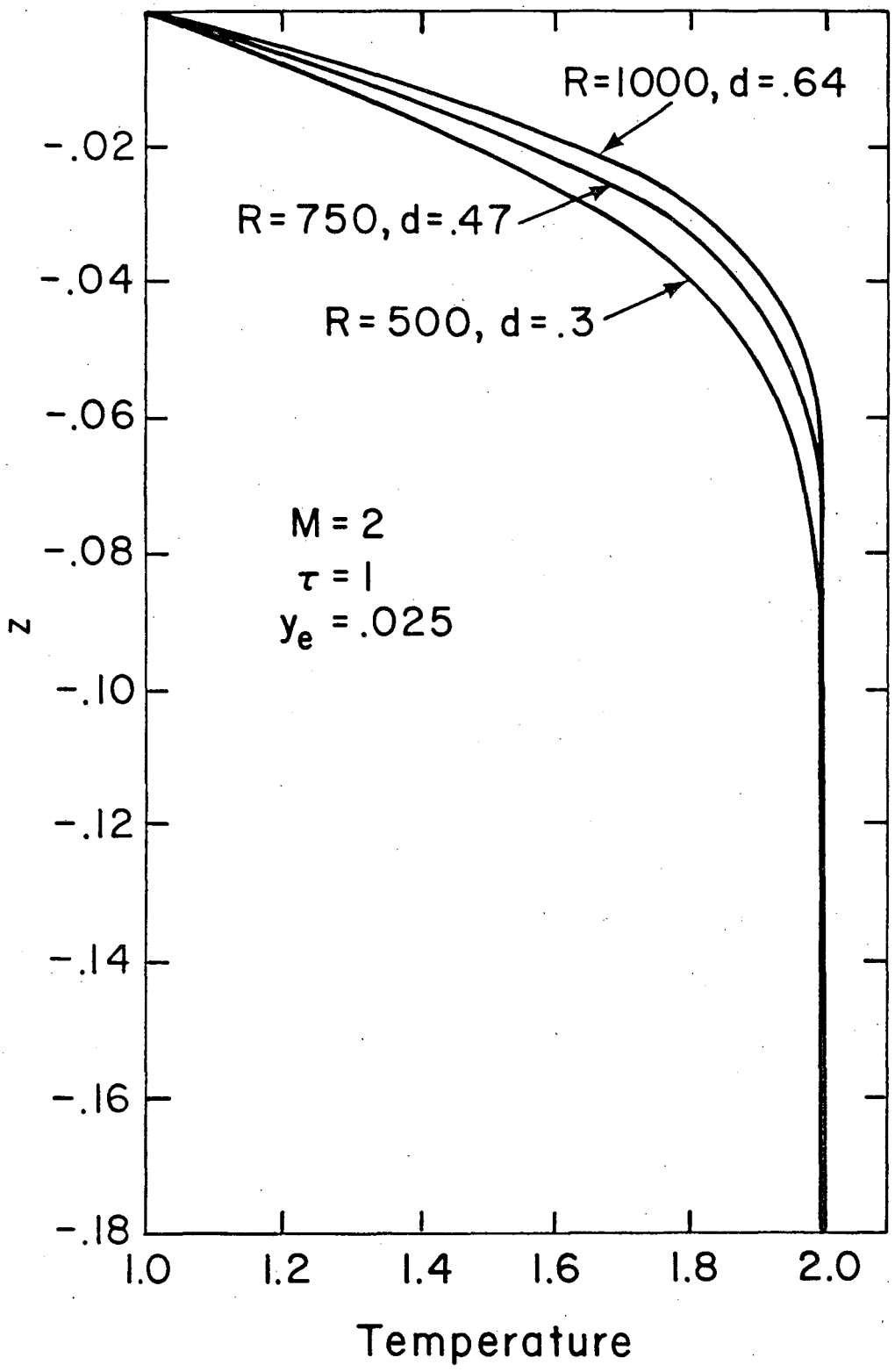

Figure 4. Effect of Rayleigh Number on the Fault Temperature at Different Depths.

XBL 796-1980

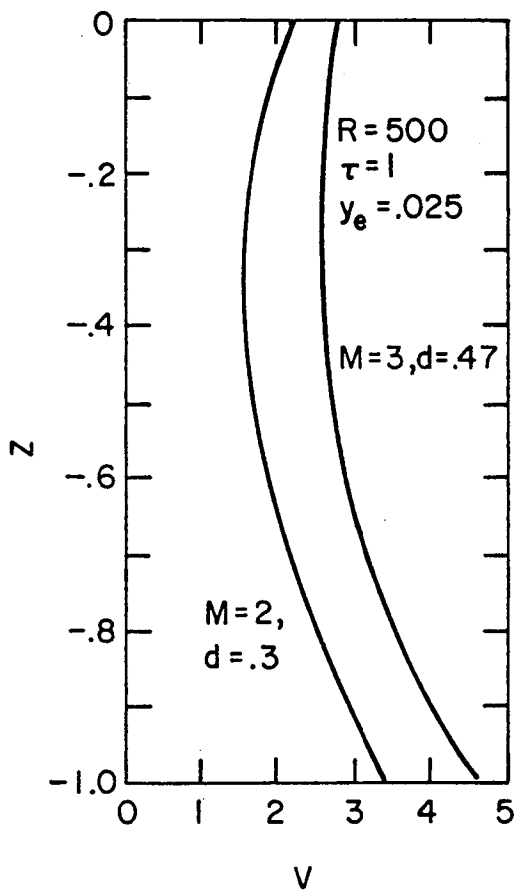

XBL796-1981

Figure 5. Horizontal Liquid Velocity in the Aquifer for Different Mass Flow Rates at Various Depths.

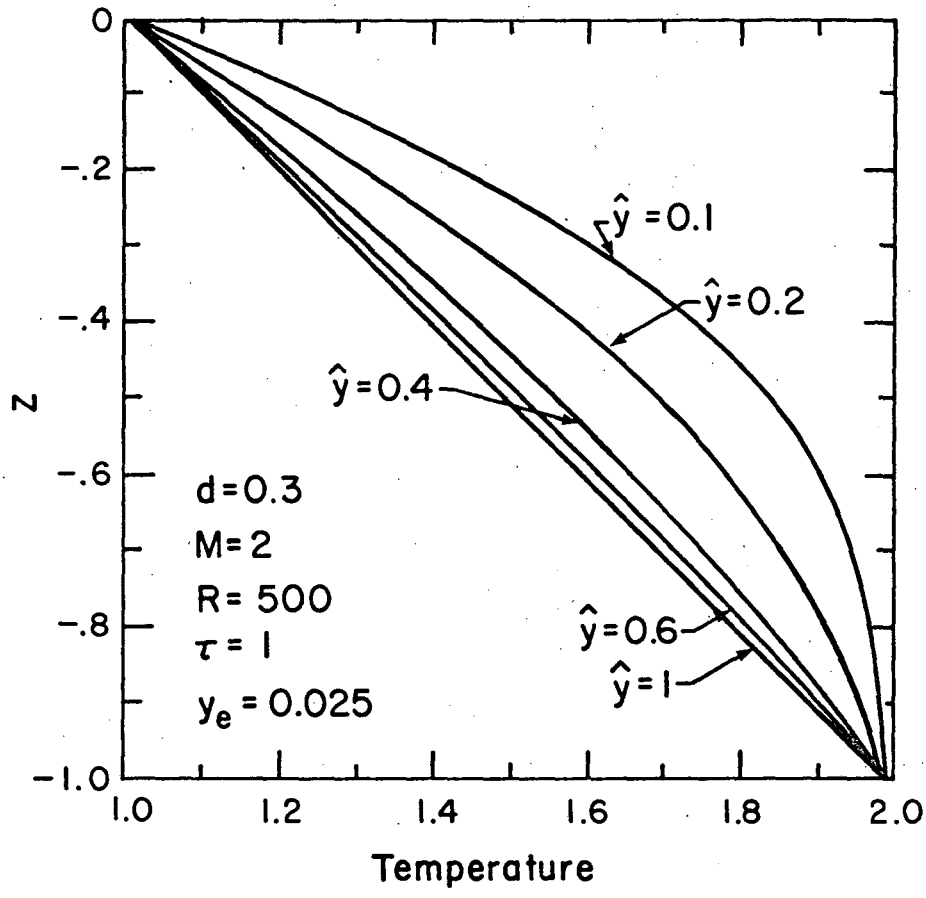

Figure 6. Temperatures in the Aquifer XBL796-1982
at Different Horizontal
Locations and Depths.

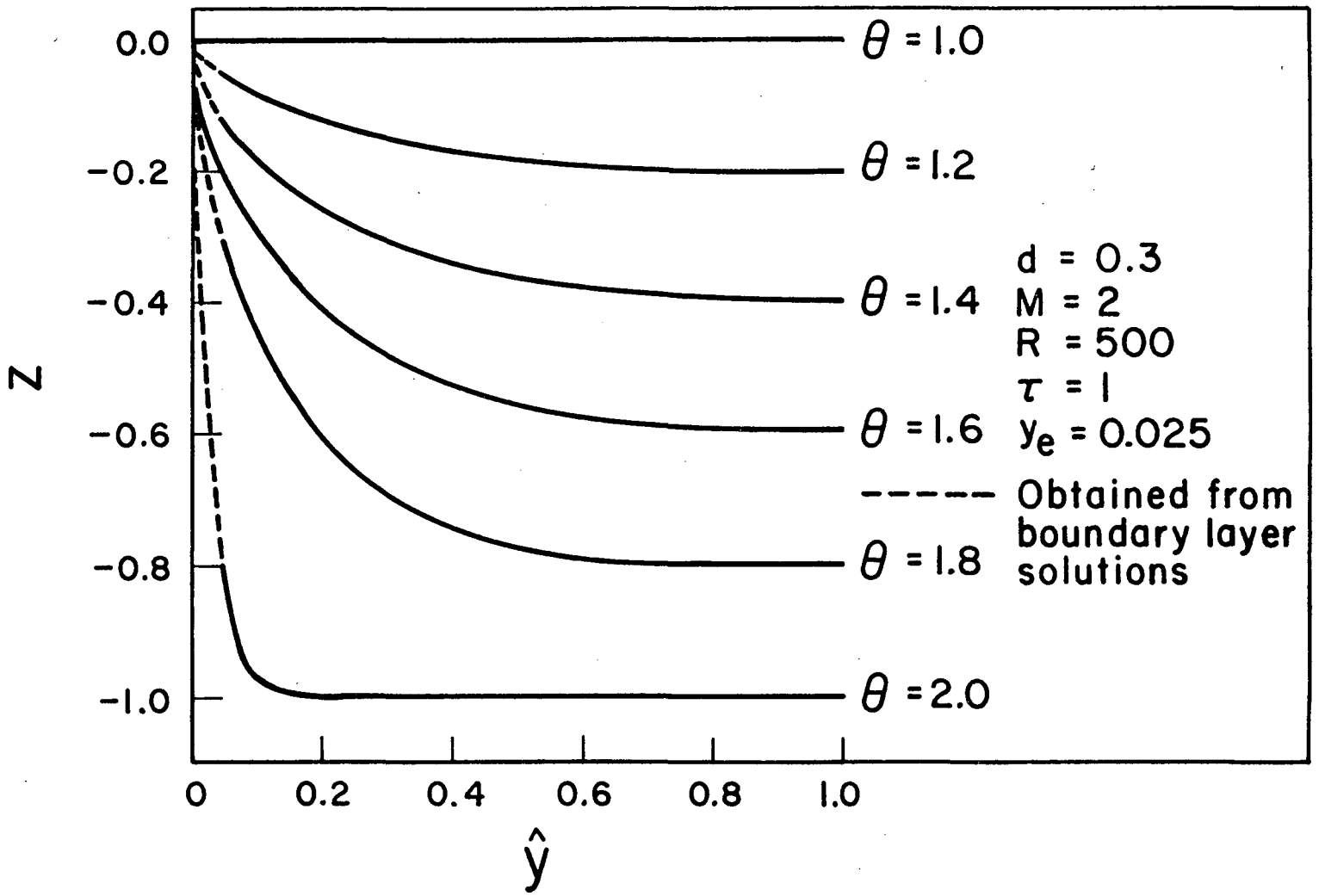

Figure 7. Isotherms in the Aquifer

XBL 796-1811

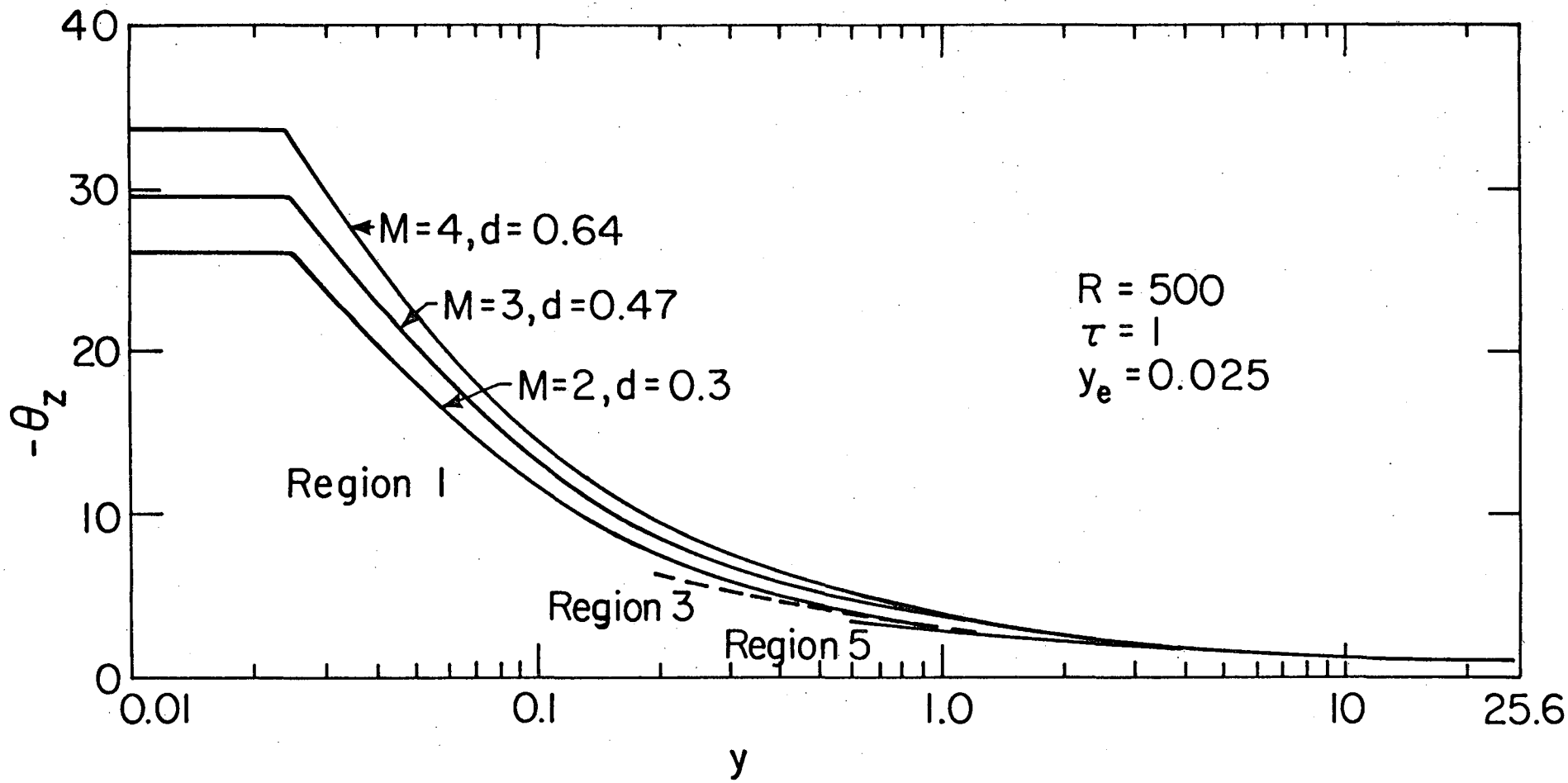

Figure 8. Effect of Mass Flow Rate on the Surface Temperature Gradients Along the Length of the Aquifer.

XBL 796-1983

the surface by an extensive region of clay rich sediments. A model of the latter system given in Goyal [1978] will be the subject of a separate paper.

6. Application to a Typical Geothermal System

This theory can be used to predict the velocities, pressures, temperatures, and heat flux at different locations in the fault and the aquifer in undeveloped systems. Let us consider a geothermal system with the following typical data:

$y_e' = 100$ m

$L' = 4$ km

$T_o' = 298$ °K.

$\Delta T' = 298$ °K

$M' = 11.72 \times 10^5$ kg/day-km length of the fault

$K' = .4 \times 10^{-9}$ cm^2

The thermal conductivity of a geothermal reservoir depends on its porosity, grain size, size distribution, physical properties of rocks and fluids, fluid saturation, temperature, and pressure etc [Martinez-Baez, L.F. 1978]. For a reservoir, associated with the interbedded shaley layers, the assumed thermal conductivity value is as follows.

$$\lambda'_m = 11.3 \times 10^4 \text{ gm - cm/sec}^3 \text{ - }^\circ\text{K}$$

using the physical properties of the water at 25°C, the following reference values can be calculated:

$q_o' = 2.94$ mm/day

$M_o' = 5.86 \times 10^5$ kg/day-km length of the fault.

The corresponding nondimensional numbers are:

$y_e = .025$

$R \approx 500$

$M \approx 2$

$\tau = 1$

$d = .3$ (Table 1), which gives $H' = 48$ km.

The plots of the horizontal velocity (mm/day) in the aquifer and the heat flux (HFU) are shown in Figures 9 and 10, repectively. The overpressure (Pascals) associated with fluid motion at fault-aquifer interface is shown in Figure 11.

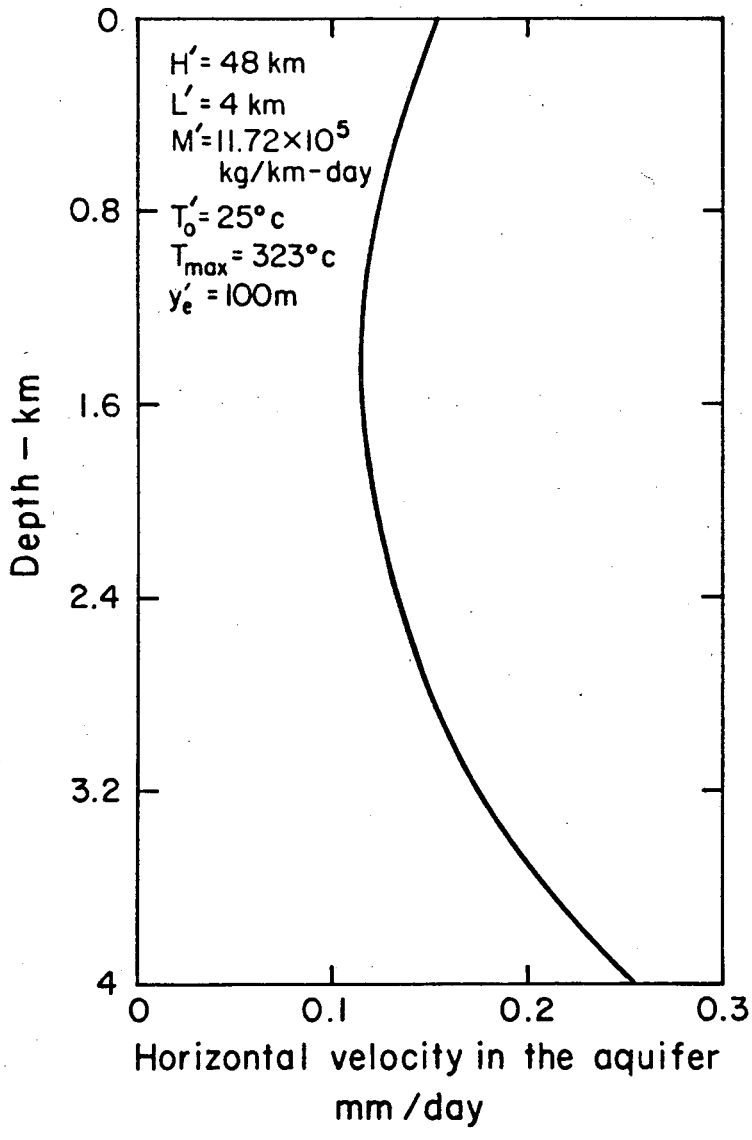

XBL 796-1984

Figure 9. Horizontal Liquid Velocity in the Aquifer at Various Depths.

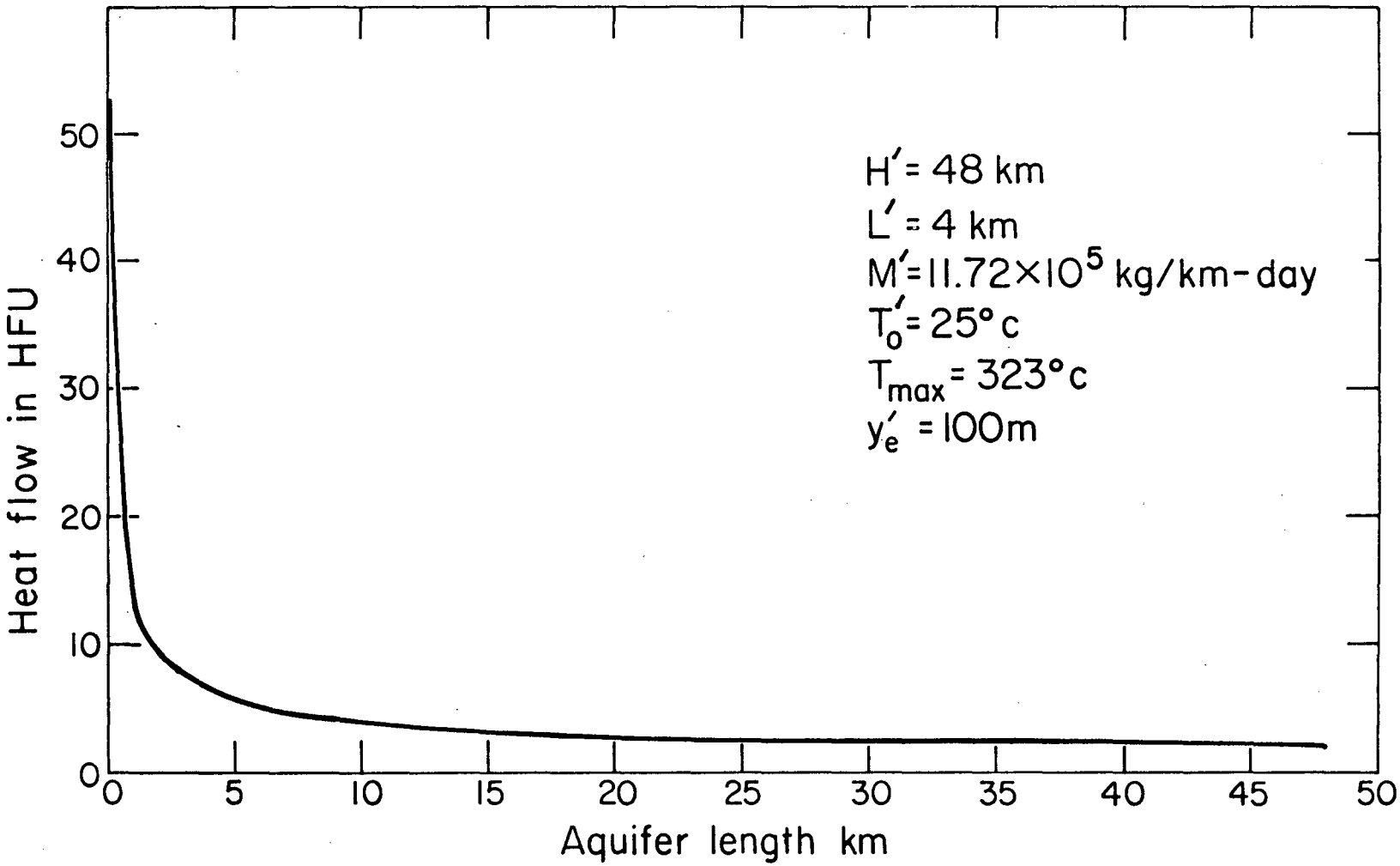

Figure 10. Surface Heat Flux along the Length of the Aquifer. XBL 796-1985

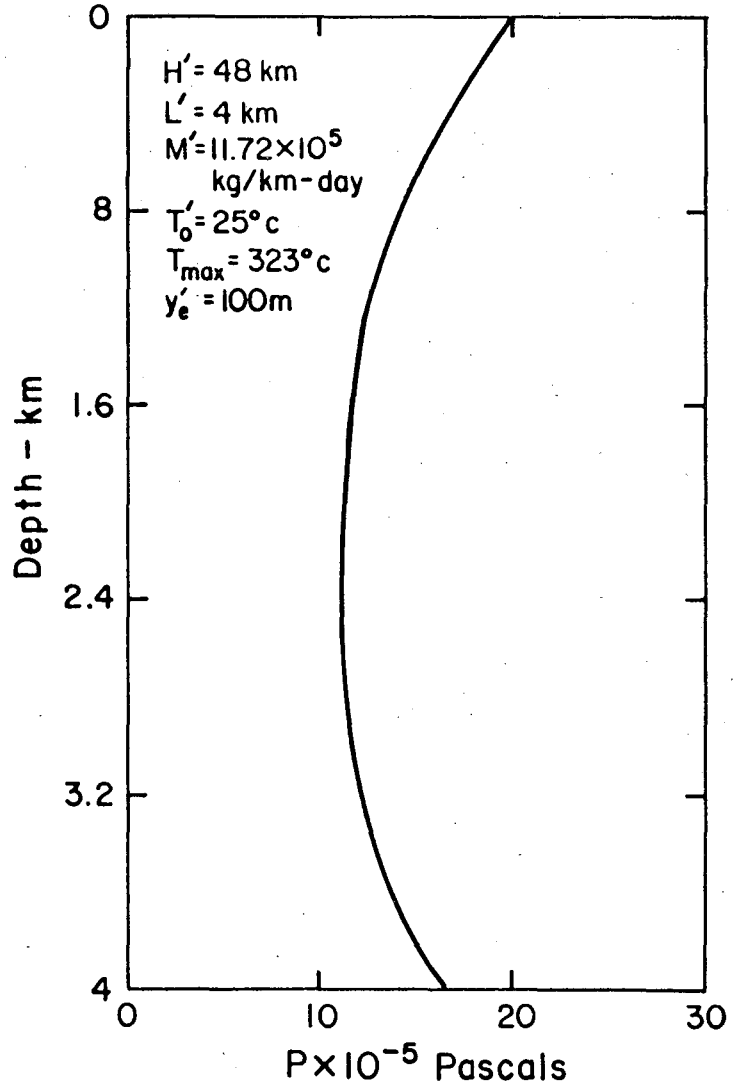

Figure 11. Fault-aquifer Interface Over Pressures at Different Depths. XBL 796 - 1986

7. Conclusions

Solutions are obtained for the velocities, pressures, temperatures, and temperature gradients in a liquid-dominated geothermal system, charged by a fault zone. Effects of various parameters such as mass flow rate, Rayleigh number, fault width is also studied on these solutions. The horizontal temperature gradients, in the near fault regions, are found to be zero, although the flow in the aquifer is purely horizontal. This idea is in contrast with the conventional wisdom that zero gradients imply upflow. Additional results for other parameter values can be found in Goyal [1978].

The concepts used to generate the model described here can be tested directly by comparison of the field data and theoretical prediction. Current measurement techniques provide surface heat flux distributions and downhole temperature distributions which can be compared with values obtained in a given model. In addition, the predicted formation pressure-depth variations could be used if accurate downhole measurements in a field were available. In this sense, three distinct measurements could be used in a variety of ways to obtain both indirect data and model verification.

ACKNOWLEDGEMENT

This work was supported by a Department of Energy contract administered by Lawrence Berkeley Laboratory.

REFERENCES

Bailey, T.P. A Hydrogeological and Subsurface Study of Imperial Valley Geothermal Anaomalies, Imperial Valley, California. Geological Sciences, University of Colorado unpublished report, 1977, 101.

Black, H.T. A Subsurface Study of the Mesa Geothermal Anomaly, Imperial Valley California. Geological Sciences, University of Colorado unpublished report, 1975, 58.

Bodvarsson, G. Physical Characteristics of Natural Heat Resources in Iceland. U.N. Conf. New Sources of Energy. Rome G.G, 1961.

Cathles, L.M. An Analysis of the Cooling of Intrusives by Groundwater Convection which Includes Boiling. Economic Geology, 1977, 72, 804-826.

Cheng, P. "Heat Transfer in Geothermal Systems," in Adances in Heat Transfer, 14, (ed. T.F. Irvine, Jr. and J.P. Hartnett) Academic Press, N.Y., 1-105. 1978.

Cheng, P., K.C. Yeung, K.H. Lau. Numberical Solutions for Steady Free Covection in an Island Geothermal Reservoir. Tech. Report #8, Hawaii Geothermal Project, University of Hawaii, 1975.

Cheng, P. and K.H. Lau. Steady State Free Convection in an Unconfined Geothermal Reservoir. J. Geophysical Research, 1974, 79,(29), 4425-4431.

Cheng, P. and W.J. Minkowicz. Free Convection about a Vertical Flat Plate Embedded in a Porous Medium with Application to Heat Transfer from a Dike. J. Geophysical Research, 1977, 82 2040-2044.

Cheng, P. and L. Teckchandani. Numerical Solutions for Transient Heating and Fluid withdrawal in a Liquid Dominated Geothermal Reservoir. J.G. Heacock (Ed.), The Earth's Crust. Geophys. Monograph #20, AGU 705-721, 1977

Combarnous, M.A. and S.A. Bories. Hydrothermal Convection in Porous Media. Advances in Hydrosciences, 1975, 10, 232-307.

Combs, J. Seismic Refraction and Basement Temperature Investigation of the East Mesa Known Geothermal Resources Area. Southern California Geothermal Resources Council, Transactions, Vol 1, May 1977, 45-47.

Combs, J. and D. Hadley. Microearthquake Investigation of the Mesa Geothermal Anomaly, Imperial Valley, California. Geophysics, 1977 42(1), 17-33.

Donaldson, I.G. A Possible Model for Hydrothermal Systems and Methods of Studying Such a Model. Third Australian Conference on Hydraulics and Fluid Mechanics, 1968, 202-204.

_____ The Simulation of Geothermal Systems with a Simple Convection Model. Geothermics, 1970, special issue 2, 649-654.

_____. Personal communication, 1978.

Eckhaus, V. "Matched Asymptotic Expansions and Singular Perturbations." Elsevier Publishing Co., Inc. New York. 1973.

Einarsson, T. The Nature of the Springs of Iceland. (in German) Rit. Visind. Esl. 26, 1, 1942.

Elder, J.W. Heat and Mass Transfer in the Earth's Hydrothermal Systems. New Zealand D.S.I.R. Bulletin #169, 1966.

Elders, W.A., R.W. Rex, T. Meidav, P.T. Robinson, and S. Biehler. Crustal Spreading in Southern California. Science, 1972, 178, 15-24.

Garg, S.K. and D.R. Kassoy. Convective Heat and Mass Transfer in Hydrothermal Systems. Geothermal Resources, (eds. L. Ryback and P. Muffler), John Wiley and Son, Ltd., London, 1979.

Goyal, K.P. Heat and Mass Transfer in a Saturated Porous Medium with Applications to Geothermal Reservoirs. PhD Thesis, Mechanical Engineering Department, University of Colorado, Boulder, 1978, p. 294.

Grindley, G.W. The Geology, Structure and Exploitation of the Wairakei Geothermal Field. Taupo, New Zealand, 1965, 131 pp.

_____ Subsurface Structures and Relation to Steam Production in the Broadlands Geothermal Field, New Zealand. Gerthermics: Proceedings of the United Nations Symposium on the Development and Utilization of Geothermal Resources, 1970, Special issue, vol. 2, part 1, 248-261.

Kassoy, D.R. and A. Zebib. Convection Fluid Dynamics in a Model of a Fault Zone lin the Earth's Crust. J. Fluid Mech., 1978, 88, 769-802.

Martinez-Baez, Luis, F. Thermal Conductivity of Core Samples from the Cerro Prieto Geothermal Field: Experimental results and an improved prediction methods. In the proceedings of the first symposium on the Cerro Prieto Geothermal Field, Baja California, Mexico, 1978, LBL Report No. 7098, University of California, Berkeley.

Mercer, J.W. and C.R. Faust. Geothermal Reservoir Simulation III: Application of Liquid and Vapor-Dominated Hydrothermal Techniques to Wairakei, New Zealand. Water Resources Research, 1979, 15 (in press).

Mercer, J.W., C.F. Pinder, and I.G. Donaldson. A Galerkin-Finite Element Analysis of the Hydrothermal System at Wairakei, New Zealand. J. of Geophysical Research, 1975, 80(17), 2608-2621.

Norton, D. Fluid Circulation in the Earth's Crust. J.G. Heacock (ed), The Earth's Crust. Geophys. Monograph #20, AGU, 1977, 693-704.

Norton, D., and J. Knight. Transport Phenomena in Hydrothermal Systems: Cooling Plutons. Amer. J. Science, 1977, 277, 937-981.

Rinehart, C.D., and D.C. Ross. Geology and Mineral Deposits of the Mount Morrison Quadrangle, Sierra Nevada, California. U.S. Geological Survey, Professional Paper No. 385, 1964, 106pp.

Riney, T.D., J.W. Pritchett, and S.K. Garg. Salton Sea Geothermal Reservoir Simulations, Proceedings, Third Workshop Geothermal Reservoir Engineering, Stanford University, Stanford, California, 1977, 178-184.

Sorey, M.L. Numerical Modeling of Liquid Geothermal Systems. Open File Report 75-613, U.S. Geological Survey, Menlo Park, California. 1975.

_____. A Model of the Hydrothermal System of Long Valley Caldera, California. Summaries, Second Workshop Geothermal Reservoir Engineering, Stanford University, Stanford, California, 1976, 324-338.

Torrence, K.E. and J.P. Sheu. Heat Transfer from Plutons Undergoing Hydrothermal Cooling and Thermal Cracking, Numerical Heat Transfer, 1978, 1, 147-160.

Turcotte, D.L., R.J. Ribando, and K.E. Torrence. Numerical Calculation of Two-Temperature Convection in a Permeable Layer with Applications to the Steamboat Springs Thermal System, Nevada. J.G. Heacock (ed.) The Earth's Crust. Geophys. Monograph #20, AGU, 1977, 722-736.

Ward, P.L. and K.H. Jacobs. Microearthquakes in the Ahuachapan Geothermal Field, El Salvador, Central America. Science, 1971, 173, 328-330.

White, D.E. Preliminary Evaluation of Geothermal Resources. U.N. Conference New Sources of Energy, Rome, G.2, 1961.

Wooding, R.A. Steady State Free Thermal Convection of Liquid in a Saturated Permeable Medium. J. Fluid Mechanics, 1957, 2, 273-285.

This report was done with support from the Department of Energy. Any conclusions or opinions expressed in this report represent solely those of the author(s) and not necessarily those of The Regents of the University of California, the Lawrence Berkeley Laboratory or the Department of Energy.

Reference to a company or product name does not imply approval or recommendation of the product by the University of California or the U.S. Department of Energy to the exclusion of others that may be suitable.

TECHNICAL INFORMATION DEPARTMENT
LAWRENCE BERKELEY LABORATORY
UNIVERSITY OF CALIFORNIA
BERKELEY, CALIFORNIA 94720